Inorganic Chemistry

pubs.acs.org/IC

Article

Metal–Metal-to-Ligand Charge Transfer in Pt(II) Dimers Bridged by Pyridyl and Quinoline Thiols

Subhangi Roy,[‡] Antonio A. Lopez,[‡] James E. Yarnell, and Felix N. Castellano*

Cite This: https://doi.org/10.1021/acs.inorgchem.1c02469

Read Online

ACCESS | Metrics & More | Article Recommendations | Supporting Information

ABSTRACT: The investigation of two distinct species of square planar dinuclear Pt(II) dimers based on *anti*-[Pt(C^N)(μ-N^S)]$_2$, where C^N is either 2-phenylpyridine (ppy) or benzo(*h*)quinoline (bzq) and N^S is pyridine-2-thiol (pyt), 6-methylpyridine-2-thiol (Mpyt), or 2-quinolinethiol (2QT), is presented. Each molecule was thoroughly characterized with electronic structure calculations, static UV–vis and photoluminescence (PL) spectroscopy, and cyclic voltammetry, along with transient absorbance and time-gated PL experiments. These visible absorbing chromophores feature metal–metal-to-ligand charge-transfer (MMLCT) excited states that originate from intramolecular d^8–d^8 metal–metal σ-interactions and are manifested in the ground- and excited-state properties of these molecules. All five molecules reported (*anti*-[Pt(ppy)(μ-Mpyt)]$_2$ could not be isolated), three of which are newly conceived here, possess electronic absorptions past 500 nm and high quantum yield PL emission with spectra extending into the far red (λ_{em} > 700 nm), originating from the charge-transfer state in each instance. Each chromophore displays excited-state decay kinetics adequately modeled by single exponentials as recorded using dynamic absorption and PL experiments; each technique yields similar decay kinetics. The combined data illustrate that pyridyl and quinoline-thiolates in conjunction with select cyclometalates represent classes of MMLCT chromophores that exhibit excited-state properties suitable for promoting light-energized chemical reactions and provide a molecular platform suitable for evaluating coherence phenomena in transient metal–metal bond-forming photochemistry.

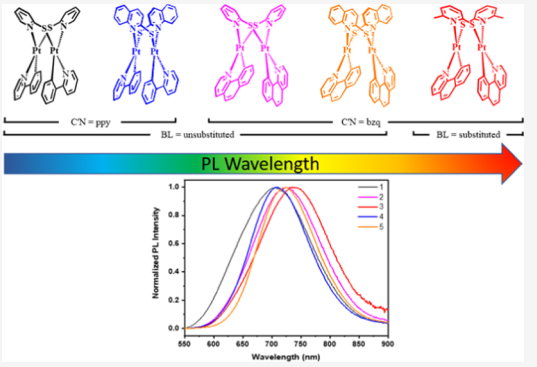

INTRODUCTION

Pt(II) transition-metal complexes featuring square planar geometries are appealing for applications ranging from photocatalysis, excited-state electron- and energy-transfer photochemistry, ion sensing, and organic light-emitting diode (OLED) technologies.[1−19] These metal–organic chromophores are valuable for their high-efficiency photoluminescence (PL) quantum yields and lifetimes, as well as their ability to systematically tune their electronic properties through structural modifications. The lowest-energy excited state of these Pt(II) complexes is typically characterized as metal-to-ligand charge transfer (MLCT) and/or ligand-to-ligand charge transfer (LLCT) as well as ligand-centered (LC) triplet character in numerous examples.[20−29] In Pt(II) complexes, the frontier d-orbital splitting renders the ligand-field states energetically inaccessible thereby eliminating a primary pathway for fast deactivation of the excited state and in turn results in highly emissive molecules at room temperature (RT). These square planar chromophores feature significant Pt–Pt interactions in the crystalline state, accounting for the wide ranges of color observed from these classes of molecular solids.[30−32] However, the metal–metal interactions that arise from simple aggregation of Pt(II) mononuclear complexes are difficult to control.[33,34] Dinuclear Pt(II) complexes, on the other hand, have well-defined molecular structures that can leverage systematically tunable metal–metal interactions, providing new classes of designer chromophores for detailed investigations of light-driven electron- and energy-transfer processes.[35]

When disposed in A-frame architectures, dinuclear Pt(II) complexes feature two pseudo-square planar coordination motifs bridged by two ligands that enable metal–metal interactions along the *z*-axis.[36−39] In the simplest qualitative molecular orbital (MO) picture, the two platinum d_{z^2} frontier orbitals overlap, producing filled dσ and dσ* molecular orbitals, as shown in Figure 1.[39] As dσ* is the highest occupied molecular orbital (HOMO), while the cyclometalating ligand π* orbital is the lowest unoccupied molecular orbital (LUMO) in this simplistic picture, the lowest-energy electronic absorptions are best characterized as metal–metal-to-ligand charge transfer (MMLCT) in character, Pt_2 dσ* → π*(C^N). The energetic splitting between the dσ and dσ*

Received: August 12, 2021

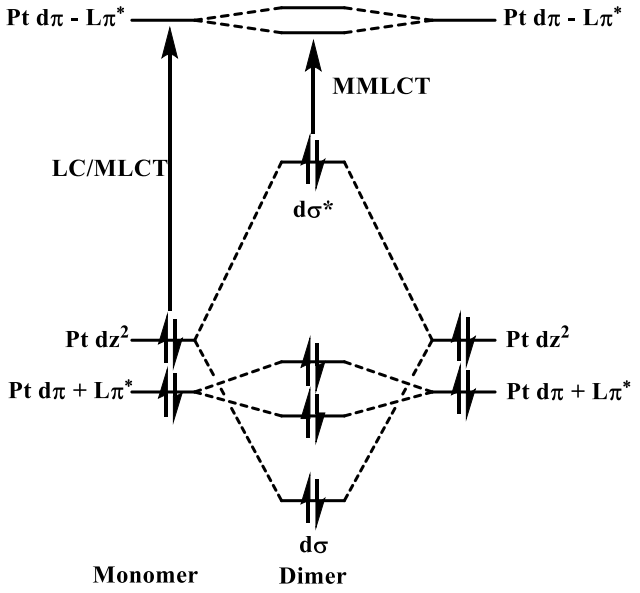

Figure 1. Simplified energy-level diagram depicting the metal−metal interactions in ligand-bridged Pt(II)−Pt(II) chromophores leading to low-energy MMLCT transitions.

orbitals is determined in part by the ground-state Pt−Pt distance, so the energy of the MMLCT transitions can be coarsely modulated by tuning this orbital overlap. This concept was first exploited by Thompson and co-workers in pyrazolate-bridged C^N terminated Pt(II) complexes, illustrating that variation in the pyrazolate 3- and 5-substituents effectively controlled the Pt−Pt separation and the nature of the electronic transitions observed.[9,39] Our research group expanded upon this effort using distinct cyclometalating ligands in concert with pyrazolate bridging ligands leading to the conclusion that judicious selection of both ligand types influences the resultant triplet character in the excited state.[40−43] The Ma group has more recently developed new classes of Pt(II) dimer chromophores featuring strikingly bright phosphorescence.[44−47] In parallel, work from Sicilia and co-workers has generated numerous examples of interesting behavior,[48−52] particularly noteworthy was the recent discovery of chameleonic photo- and mechanoluminescence response from NHC cyclometalated Pt(II) dimers.[53]

The structural effects leading to MMLCT excited-state characters in platinum dimers deserve further consideration as these design features are critical toward developing molecules featuring long lifetimes that can be systematically tuned through subtle geometry changes. Pyrazolate bridging ligands nominally represent symmetric 3−5-substituted N^N-type ligands valuable for constructing Pt(II) dimers with MMLCT excited states, whereas asymmetric pyridine derivatives including 6-substituted-2-hydroxypyridines (N^O),[54] 2-mercaptopyridines (N^S),[37,38,55−57] and 2-mercaptobenzothiazoles have also realized success.[58] For example, Kato and co-workers prepared a Pt(II) dimer featuring pyridine-2-thiolate bridges and 2-phenylpyridine (ppy), culminating in **1** (Figure 2), exhibiting triplet MMLCT character in the emitting state.[37] The primary focus of their study was to illustrate how the photoluminescence properties of these molecules could be turned off and then back on again using oxidative addition and reductive elimination of halogens.[37] More recent work investigated the vibrational wavepacket dynamics of **1** using ultrafast degenerate pump-probe transient absorption spectroscopy, which demonstrated that the low-frequency Pt−Pt vibrational stretching motion was found to have strong coherent oscillations during excited-state decay as a result of strong π-interactions between the two cyclometalating ligands.[59] This particular molecule was selected since its ground-state absorption spectrum sufficiently overlapped the femtosecond laser's broad spectral output, enabling the study of coherence in the first place. The current study seeks to provide a broader platform of molecules for understanding how the vibrational coherence in **1** would be impacted by modulation of the ligand structures, the metal bonded heteroatoms, and the geometric changes resulting from these substitutions. Due to the nature of such ultrafast experiments, related MMLCT chromophores need to be designed so that their low-energy absorption bands appropriately overlap the spectrum provided by the compressed laser pulses.[59] Although there are numerous examples of MMLCT chromophores throughout the literature, most feature visible absorption bands in the blue and longer wavelength transitions are necessary to test coherence effects in these molecules. Importantly, Pt(II) dimers featuring photoinduced structural rearrangements are also amenable to femtosecond electron diffraction enabling visualization of its molecular motion,[60] and such experiments would benefit from chromophores possessing long-wavelength absorption bands better suited for pumping with highly compressed laser pulses.

We recently reported a complete synthesis and photophysical study on antidisposed dinuclear Pt(II) molecules that exhibit a low-energy MMLCT excited state with 2-hydroxypyridine derivatives serving as the bridging ligands. The 2-

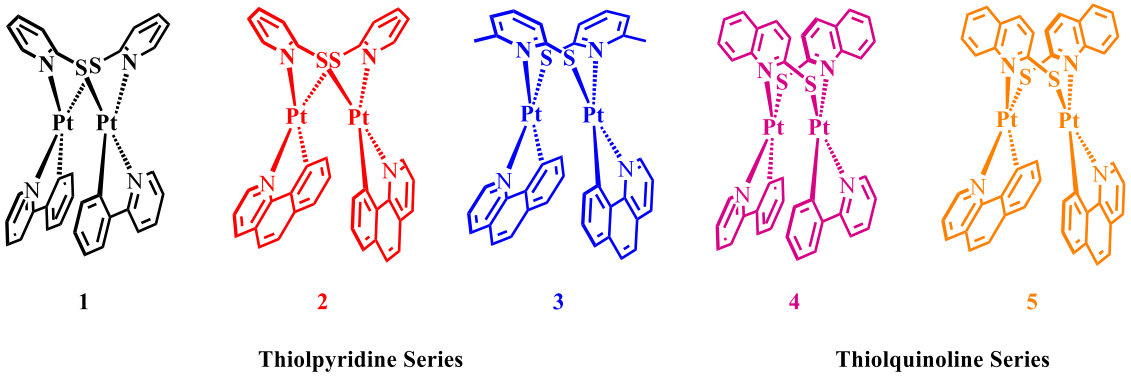

Figure 2. Structures of the thiolpyridine and thiolquinoline containing MMLCT chromophores.

https://doi.org/10.1021/acs.inorgchem.1c02469
Inorg. Chem. XXXX, XXX, XXX−XXX

Scheme 1. Generalized Synthetic Scheme for the N^S Bridged Platinum(II) Complexes[a]

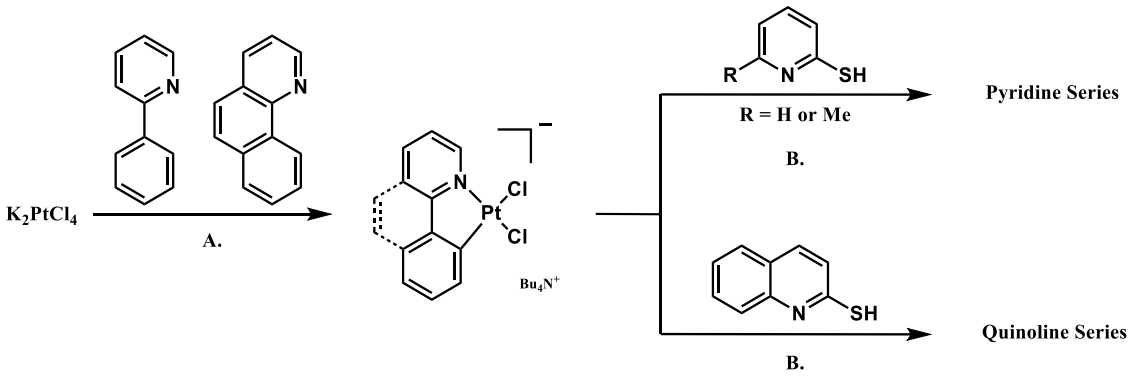

[a]Reagents and conditions: (A) dichloromethane/methanol at 50 °C for 24 h. (B) Acetonitrile/tributylamine in ethanol at RT for 24 h.

hydroxypyridine-based Pt(II) dimers were able to produce the shortest reported metal−metal distance (2.8155(3) Å) across all Pt(II)-based MMLCT chromophores while exhibiting distinct low-energy absorbances >500 nm and PL spectra with maxima >700 nm.[54]

Building upon our previous results seeking to identify long-wavelength absorbing MMLCT chromophores in conjunction with the work of Kato, we synthesized a set of Pt(II) dimers wherein both the cyclometalating and bridging ligands were varied (Figure 2). These dimers are composed as *anti*-[Pt(C^N)(μ-N^S)]$_2$, where C^N is 2-phenylpyridine (ppy) or benzo(*h*)quinoline (bzq) and N^S is pyridine-2-thiol (pyt), 6-methylpyridine-2-thiol (Mpyt), or 2-quinolinethiol (2QT). The dimers in the thiolpyridine series demonstrate how the MMLCT energetics are influenced by the sterics imposed by the bridging ligands as well the specific C^N ligand. Similarly, the thiolquinoline series is composed of two molecules that modulate the energy of the LUMO by varying the cyclometalating ligand. All molecules reported herein were prepared as anti-isomers (based on the relative orientation of the C^N and bridging ligands), confirmed by ^{1}H and ^{13}C NMR spectroscopy. Unfortunately, all attempts to produce single X-ray quality crystals of the newly reported molecules were unsuccessful. Consistent with previously reported Pt(II) dimers, isolation of the single anti-isomer in each case was likely a result of the trans-influence imposed by each cyclometalating subunit and the asymmetric nature of the bridging ligands. All five molecules feature electronic spectra extending beyond 500 nm and long-wavelength photoluminescence (PL) with high quantum yields (up to 16%) emitting from their long-lifetime MMLCT excited states (λ_{PL} > 700 nm) extended in comparison to our hydroxypyridine-based dimers.[54] The combined data illustrate that pyridyl- and quinoline-thiolates in conjunction with appropriate cyclometalating ligands yielded new long-wavelength absorbing MMLCT chromophores possessing suitable photophysical properties for photosensitizing excited-state reactions as well as providing a molecular platform where vibrational coherence phenomena resulting from transient metal−metal bond formation can be systematically investigated.

EXPERIMENTAL SECTION

Reagents and Chemicals. Standard Schlenk techniques were used for preparing all molecules under an inert atmosphere using dry nitrogen gas. The commercially available chemicals used for all syntheses were purchased from VWR and used without further purification. The intermediates, [Pt(ppy)Cl$_2$]Bu$_4$N and [Pt(bzq)Cl$_2$]-Bu$_4$N, were prepared in accord with their published protocols and resulted in ^{1}H NMR and mass spectra that quantitatively matched published values.[38,61−63] Samples used for optical spectroscopy were prepared using toluene (spectroscopic-grade) and were deaerated using the freeze−pump−thaw technique.[64]

Synthesis of [Pt(N^C)(μ-N^S)]$_2$ Complexes. The syntheses of these molecules were performed by following synthetic procedures of those published previously.[37,38] The generalized approach for the synthesis of both series of Pt(II) dimers is presented in Scheme 1. Briefly, the [Pt(ppy)Cl$_2$]Bu$_4$N or [Pt(bzq)Cl$_2$]Bu$_4$N intermediate was dissolved in 20 mL of acetonitrile (~10 mM) with 1.25 equiv of the respective thiol-substituted bridging ligand, followed by the addition of Bu$_3$N in ethanol. The stirred reaction mixture was maintained at RT for 24 h under a N$_2$ atmosphere. The product precipitated out of the solution and the solid was collected by vacuum filtration through a coarse frit and the collected solid was rinsed with acetonitrile. All Pt(II) dimers were isolated in the form of the anti-isomer as the exclusive product. *anti*-[Pt(ppy)(μ-Mpyt)]$_2$ could not be isolated using this protocol.

anti-[Pt(ppy)(μ-pyt)]$_2$ ***(1)***. Yield: 32% (60 mg). ^{1}H NMR (400 MHz, dimethyl sulfoxide (DMSO)-d_6) δ 8.50 (d, J = 4.7 Hz, 2H), 7.78−7.68 (m, 2H), 7.61 (d, J = 5.1 Hz, 2H), 7.40 (t, J = 8.1 Hz, 4H), 7.33−7.24 (m, 2H), 7.22−7.07 (m, 4H), 7.03 (d, J = 6.6 Hz, 2H), 6.94−6.85 (m, 2H), 6.65 (t, J = 6.9 Hz, 2H), 6.33 (t, J = 7.4 Hz, 2H). Matrix-assisted laser desorption ionization time-of-flight mass spectrometry (MALDI-TOF MS): Found m/z 918.072 (M + H$^+$). Calcd for $C_{32}H_{25}N_4S_2{}^{194}Pt_2$ 918.07. The ^{1}H NMR spectrum and the single-crystal X-ray structure quantitatively matched the prior report.[37]

anti-[Pt(bzq)(μ-pyt)]$_2$ ***(2)***. Yield: 31% (93 mg) ^{1}H NMR (400 MHz, CD_2Cl_2) δ 8.70 (d, J = 5.8 Hz, 2H), 7.97 (dd, J = 8.0, 6.7 Hz, 4H), 7.59 (d, J = 8.4 Hz, 2H), 7.39−7.05 (m, 10H), 6.99−6.70 (m, 4H), 6.53 (t, J = 7.6 Hz, 2H). ^{13}C NMR (176 MHz, DMSO-d_6) δ 170.18, 153.98, 152.07, 146.27, 139.93, 138.20, 136.80, 134.77, 131.85, 130.19, 128.00, 126.76, 125.90, 122.49, 121.00, 119.47, 118.33, 118.09. MALDI-TOF MS: Found m/z 966.092 (M + H$^+$). Calcd for $C_{36}H_{25}N_4S_2{}^{194}Pt_2$ 966.07.

anti-[Pt(bzq)(μ-Mpyt)]$_2$ ***(3)***. Yield: 35% (78 mg) ^{1}H NMR (400 MHz, DMSO-d_6) δ 8.30 (d, J = 7.8 Hz, 2H), 7.81 (d, J = 4.8 Hz, 2H), 7.60−7.43 (m, 2H), 7.42−7.17 (m, 8H), 7.00 (d, J = 7.2 Hz, 2H), 6.90 (d, J = 7.2 Hz, 2H), 6.66 (d, J = 7.8 Hz, 2H), 6.20 (t, J = 7.6 Hz, 2H), 2.97 (s, 6H). ^{13}C NMR (176 MHz, DMSO-d_6) δ 170.26, 158.90, 154.88, 146.46, 140.63, 139.70, 136.97, 135.79, 132.34, 129.80, 128.63, 126.93, 126.69, 126.44, 122.89, 121.52, 119.69, 119.57, 26.25. MALDI-TOF MS: Found m/z 994.136 (M + H$^+$). Calcd for $C_{38}H_{29}N_4S_2{}^{194}Pt_2$ 994.11.

anti-[Pt(ppy)(μ-2QT)]$_2$ ***(4)***. Yield: 31% (113 mg) ^{1}H NMR (400 MHz, CD_2Cl_2) δ 9.85 (d, J = 8.7 Hz, 2H), 7.70−7.37 (m, 14H), 7.37−7.24 (m, 2H), 7.17 (d, J = 7.8 Hz, 2H), 6.97 (d, J = 7.7 Hz, 2H), 6.81−6.62 (m, 4H), 6.44 (dd, J = 10.4, 4.5 Hz, 2H). ^{13}C NMR

https://doi.org/10.1021/acs.inorgchem.1c02469
Inorg. Chem. XXXX, XXX, XXX−XXX

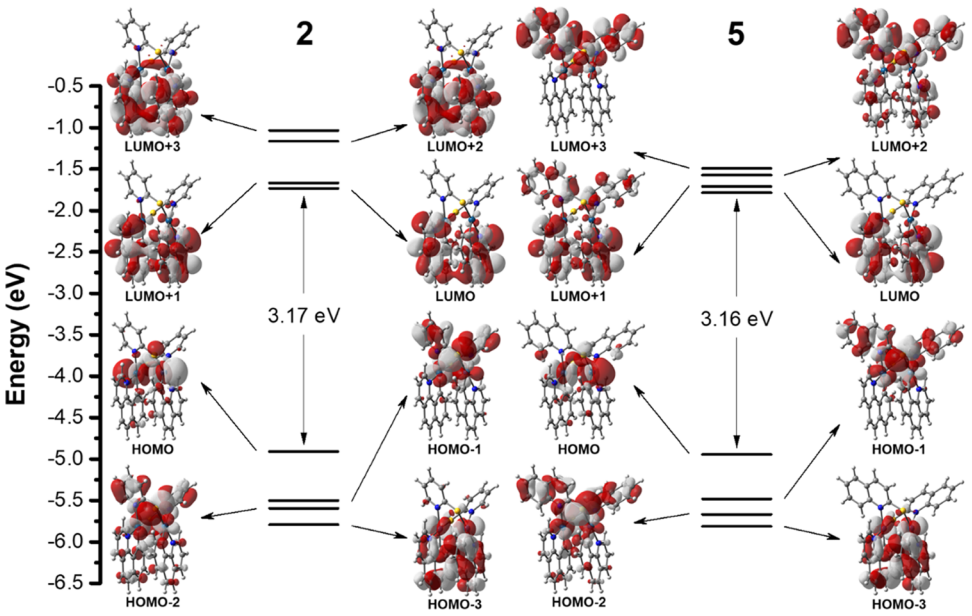

Figure 3. Frontier molecular orbital diagram of the pyridine and quinoline series of molecules using **2** and **5** as representative examples, calculated at the PCM-PBE0-D3/Def2-SVP/SDD level of theory.

(176 MHz, DMSO-d_6) δ 165.98, 155.98, 147.46, 147.34, 144.57, 143.51, 137.37, 134.08, 132.71, 128.64, 128.57, 128.51, 127.47, 126.87, 126.05, 124.45, 122.92, 121.92, 121.56, 118.52. MALDI-TOF MS: Found m/z 1018.137 (M + H$^+$). Calcd for $C_{40}H_{29}N_4S_2{}^{194}Pt_2$ 1018.11.

anti-[Pt(bzq)(μ-2QT)]$_2$ (**5**). Yield: 49% (178 mg) ^{1}H NMR (400 MHz, CD_2Cl_2) δ 9.86 (d, J = 8.8 Hz, 2H), 7.85 (d, J = 8.2 Hz, 2H), 7.63 (dd, J = 17.0, 8.9 Hz, 8H), 7.53 (d, J = 7.3 Hz, 2H), 7.42 (t, J = 7.8 Hz, 2H), 7.30 (t, J = 7.5 Hz, 2H), 7.23 (d, J = 8.7 Hz, 2H), 7.11 (d, J = 8.7 Hz, 2H), 7.02−6.94 (m, 2H), 6.84 (d, J = 7.7 Hz, 2H), 6.63 (t, J = 7.6 Hz, 2H). ^{13}C NMR (176 MHz, DMSO-d_6) δ 172.77, 154.28, 147.44, 146.47, 140.25, 140.07, 137.50, 133.68, 132.39, 130.83, 129.43, 128.78, 128.64, 128.45, 127.31, 126. 97, 126.38, 125.68, 125.17, 123.02, 121.58, 120.43. MALDI-TOF MS: Found m/z 1066.171 (M + H$^+$). Calcd for $C_{44}H_{29}N_4S_2{}^{194}Pt_2$ 1066.11.

General Techniques. A Varian Inova 400 NMR spectrometer operating at 400 MHz was used to record all ^{1}H NMR spectra. Residual solvent protons were used to reference the NMR chemical shifts, and the splitting patterns were assigned as s (singlet), d (doublet), t (triplet), and m (multiplet). ^{13}C NMR spectra were recorded on a Bruker Avance Neo 700 MHz NMR spectrometer. All chemical shifts were referenced to residual solvent signals. MALDI-TOF mass spectrometry measurements were performed in the Molecular Education, Technology, and Research Innovation Center (METRIC) at North Carolina State University. A Shimadzu UV-3600 spectrometer was used for recording all of the electronic spectra. Static photoluminescence spectra were recorded on an Edinburgh FS920 spectrofluorometer. Absolute quantum yields of each compound were measured on deaerated samples prepared in a N_2-filled glovebox and recorded with an FS5 fluorometer (Edinburgh Instruments) equipped with an integrating sphere. Solutions of compounds with absorbances ranging between 0.1 and 0.2 OD at the excitation wavelength (500 nm) were used for all photoluminescence measurements.

Electrochemistry. Electrochemical experiments took place inside a N_2-filled glovebox (MBraun) in concert with a CH Instruments model 600E series potentiostat. Cyclic voltammetry and differential pulse voltammetry (CV and DPV) of the complexes were recorded in a 1:1 acetonitrile:toluene mixture with added tetrabutylammonium hexafluorophosphate ($TBAPF_6$) (0.1 M) as the supporting electrolyte. In a three-electrode arrangement, a platinum disk, a platinum wire, and $Ag/AgNO_3$ were used as the working electrode, counter electrode, and reference electrode, respectively. Measurements were performed using a 100 mV/s scan rate with applied potentials observed relative to ferrocenium/ferrocene (Fc^+/Fc) as an internal standard [$E_{1/2}/(Fc^+/Fc)_{obsd}$ = 0.078 ± 0.005 V vs $Ag/AgNO_3$].[65]

Nanosecond Transient Absorption Spectroscopy. Nanosecond transient absorbance experiments were executed using an LP920 instrument (Edinburgh Instruments) at room temperature. Briefly, a tunable Vibrant 355 Nd:YAG/OPO laser (OPOTEK) generated the exciting nanosecond laser pulse and a pulsed xenon arc lamp produced the probe light. An iStar ICCD camera (Andor Technologies) was used to collect all transient absorption difference spectra, which was controlled by the LP920 software. All samples were deaerated using three freeze−pump−thaw cycles and measured in quartz optical cells of pathlength = 1 cm. Optical densities between 0.3 and 0.8 were used for all samples at the excitation wavelength (λ_{ex} = 500 nm; 2.0 mJ/pulse). To increase the signal-to-noise ratio, all reported kinetic traces and difference spectra were averaged over 100 laser shots. To ensure that the samples did not degrade during the experimental acquisitions, ground-state absorption spectra before and after each experiment were recorded. The fitting routines available in the Origin Pro 8 software package were utilized to evaluate the single wavelength transient kinetic data.

Computational Details. Electronic structure calculations on **1**−**5** were determined using the Gaussian 09 software package (revision D.01)[66] and the computational resources of the North Carolina State University HPC. Ground-state geometry optimizations and time-dependent-density functional theory (TD-DFT) calculations were performed on the ground- and lowest triplet-state using the B3LYP,[67,68] M06,[69] and PBE0 functional,[70] with the Def2-SVP basis set on all atoms,[71] except for the platinum core electrons, which were simulated using the Stuttgart−Dresden effective core potentials (ECP).[72] The polarizable continuum model (PCM) mimicked the toluene solvent environment.[73] A GD3 dispersion correction was applied to all minimized structures.[74] Frequency calculation performed on all ground- and triplet-state minimized structures did not generate any imaginary frequencies. The ground-state geometries of similarly structured pyridine and thiolpyridine dimers were benchmarked using M06-D3 and PBE0-D3 functionals having the closest results to that of the crystal structures.[37,54] Energies and oscillator strengths were calculated for the 50 lowest singlet and 10 lowest triplet excitations using time-dependent DFT calculations.

https://doi.org/10.1021/acs.inorgchem.1c02469
Inorg. Chem. XXXX, XXX, XXX−XXX

RESULTS AND DISCUSSION

Synthesis and Structural Characterization. Compounds **1**−**5** were prepared using adaptations of established synthetic protocols.[37,38] All isolated products were in the anti-configuration, which was verified by ^{1}H and ^{13}C NMR spectroscopy. MALDI-TOF MS was consistent with the structures rendered in Figure 2.

Electronic Structure Calculations. To obtain insight about the ground and excited states in these chromophores, DFT and TD-DFT calculations were performed on **1**−**5** employing the PBE0-D3/Def2-SVP level of theory using PCM (toluene), an ultrafine grid, and tight convergence criteria. This level of theory was chosen due to previous benchmarking efforts comparing the crystal structures of analogous Pt dimers published previously to optimized structures using B3LYP, M06, and PBE0 functionals with and without dispersion correction in the vapor phase.[37,54] By comparing overall structure and Pt−Pt distances, it was determined that the M06 functional had the closest match to crystal structures when no dispersion correction was used (Table S1). However, when the three functionals were subjected to the GD3 dispersion correction, all of them improved with the PBE0-D3 functional having the closest Pt−Pt distances and overall structures with respect to the previously published crystal structures (Table S2).

The optimized ground-state molecular structures (for **1**−**5**) and the calculated frontier MOs for **2** and **5** are presented in Figure 3 and those of the remaining molecules are available in the Supporting Information (SI). The HOMO, LUMO, and LUMO + 1 echo those calculated in **1**−**3**, suggesting that the electronic structure insignificantly changes through variation of the bridging and C^N ligands. Molecules **4** and **5** are similar to **1**−**3** but have additional LUMO and LUMO + 1 contributions arising from the 2-thiolquionoline bridging ligand. In all instances, the HOMO resides on antibonding d_{z^2} orbitals of the two platinum atoms, reminiscent of the dσ* MO resulting from the Pt−Pt σ-interaction. This is also supported through the calculated Pt−Pt distances for the optimized ground state for all five complexes. These all fall between 2.86 and 2.87 Å, resulting in the significant overlap between the two Pt d_{z^2} orbitals (Table S2). The LUMO and LUMO + 1 MOs are the in- and out-of-phase π* combination of the C^N ligand used. The LUMO of **4** and LUMO + 1 of **4** and **5** reside on both cyclometalating and bridging ligands suggesting near energetic degeneracy of these orbitals.

To evaluate the structural distortions of these long-lived excited states, the geometry of the lowest triplet was adjusted at the PCM-PBE0-D3/Def2-SVP/SDD level. In all five molecules, the calculated Pt−Pt distance of the triplet state was 2.67−2.68 Å, a reduction of ∼0.19 Å from their optimized ground-state structures. Since the lowest-energy excited state of these molecules is anticipated as MMLCT in character,[42,59,75] the electron density in the Pt−Pt dσ* molecular orbital is significantly reduced in the triplet excited state. This increases the strength of the interaction between the two platinum atoms, effectively driving them closer together.

Electrochemistry. The electrochemical properties of **1**−**5** were measured through cyclic voltammetry (CV) and differential pulse voltammetry (DPV). As the molecules have limited solubility in a single solvent, measurements were conducted in a mixture of acetonitrile and toluene (1:1) with 0.1 M $TBAPF_6$ as the supporting electrolyte. The redox potentials determined in **1**−**5** are collected in Table 1 and the corresponding cyclic and differential pulse voltammograms are provided in Figures S1−S5.

Table 1. Electrochemical Data for 1−5 Measured In Acetonitrile:Toluene (1:1) with 0.1 M $TBAPF_6$[a]

complex	$E_{(1/2)}$(ox)[b] (V)	$E_{(1/2)}$(red)[b] (V)
1	−0.099	−2.43
2	−0.082	−2.31
3	−0.039	−2.26
4	0.068	−2.38
5	0.056	−2.29

[a]Potential values are reported vs Fc^+/Fc. Scan rate = 100 mV/s. [b]All peaks are irreversible in cyclic voltammetry.

All Pt(II) dimers investigated here exhibit irreversible one-electron reduction waves in cyclic voltammetry experiments. Complexes **1**−**5** have reduction potentials that range from −2.26 to −2.43 V with reduction potential values that are similar when constructed from the same cyclometalating ligand; for example, **1** and **4** featuring 2-phenylpyridine (ppy) have reduction potentials within the experimental error of each other as do **2**, **3**, and **5** corresponding to bzq cyclometalates. Molecules with ppy (**1** and **4**) have more negative reduction potentials with respect to those with bzq (**2**, **3**, and **5**), assumed to result from increased stabilization of the electron in the conjugated bzq ring system. The irreversibility of the one-electron reductions has been observed in related molecules and these findings are not surprising.[29,40,54,76] These molecules also exhibited irreversible one-electron oxidation processes, as observed in their cyclic voltammograms measured in a 1:1 mixture of acetonitrile:toluene (Table 1). The irreversible nature of the oxidations likely results from nucleophilic attack by CH_3CN, possibly resulting in permanent oxidative addition products.[29,54,77]

Electronic Spectroscopy. The electronic spectra of both series of dimer molecules in toluene are presented in Figure 4 with all germane experimental data collected in Table 2. In both series of chromophores, the high-energy and strongly absorbing transitions below 350 nm are assigned to ligand-centered (LC) $\pi \rightarrow \pi$* transitions, as determined by direct comparison with the absorption profiles of the free ligands. The absorption features near 400 nm in all cases are attributed to transitions within the bridging thiol ligand (pyt, Mpyt, or 2QT) (Figures S6 and S7). Molecules **1**−**5** also exhibit low-energy (above 500 nm) and weakly absorbing (∼3000 M^{-1} cm^{-1}) transitions assigned as MMLCT in character. As discussed earlier, these assignments are supported by DFT calculations (Figures S33−S37), which suggest that the lowest-energy transitions in these molecules are Pt_2 σ* $\rightarrow$ π* (ppy or bzq). The broad and featureless MMLCT absorption band features maxima at 508 nm (**1**), 512 nm (**2**), 542 nm (**3**), 518 nm (**4**), and 530 nm (**5**). The molecules where bzq is the cyclometalating ligand (**2**, **3**, and **5**) have the lowest-energy transitions, consistent with more extended π-conjugation in bzq. Of the molecules in the thiolpyridine series, **3** is lowest in energy, likely due to the 6-methyl substituent resident on the bridging thiol, decreasing the Pt−Pt interaction thereby raising the energy of the σ* orbital (HOMO). We note that single-crystal X-ray determinations could not be obtained for **2**−**5** that would have provided experimental ground-state Pt−Pt

https://doi.org/10.1021/acs.inorgchem.1c02469
Inorg. Chem. XXXX, XXX, XXX−XXX

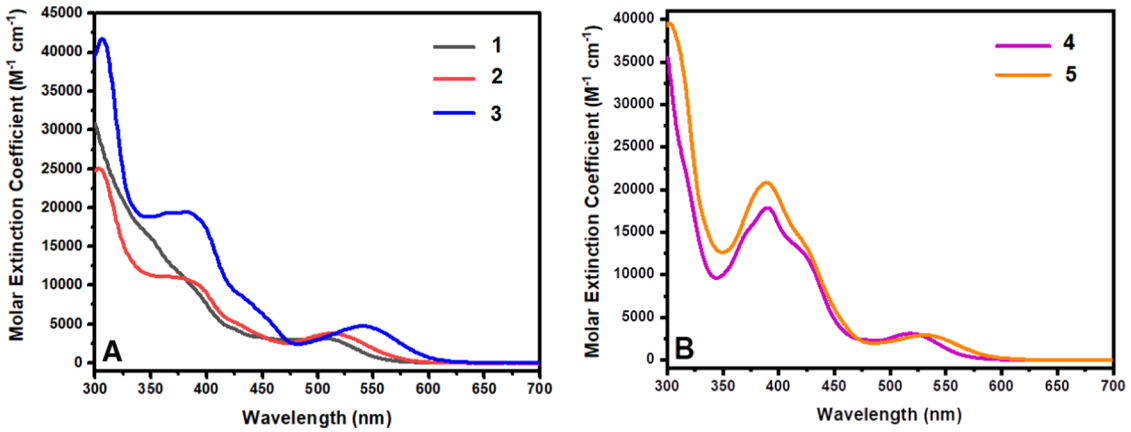

Figure 4. UV−vis absorption spectra of **1** (black), **2** (red), and **3** (blue) (A) and **4** (magenta) and **5** (orange) (B) measured in toluene at room temperature.

Table 2. Spectroscopic[a] and Photophysical Properties of the Pt(II) Dimers

complex	λ_{Abs} (nm)[b] (ε, M^{-1} cm^{-1})	λ_{em} (nm)[b]	Φ_{em} (%)[c]	λ_{em} (nm) (77 K)	τ_{em} (μs) (RT, 77 K)	τ_{TA} (μs)	k_r[d] ($\times 10^{-4}$ s^{-1})	k_{nr}[e] ($\times 10^{-6}$ s^{-1})
1	300 (29 200), 370 (11 800), 508 (3460)	706	16	630	1.1, 4.9	1.1	14.5	0.76
2	304 (31 800), 380 (12 900), 512 (3280)	725	9.5	654	0.63, 5.4	0.64	15.1	1.43
3	305 (41 800), 366 (20 100), 542 (4650)	736	8.3	658	0.51, 5.2	0.50	16.2	1.79
4	300 (31 500), 389 (17 900), 518 (3100)	710	1.3	625	0.10, 4.7	0.095	13.0	9.87
5	301 (39 600), 389 (20 900), 530 (2900)	725	10.4	636	0.72, 5.9	0.720	14.4	1.24

[a]Room-temperature (RT) and 77 K measurements were performed in toluene. [b]Absorption and emission maxima, ±2 nm. [c]Absolute quantum yield measurements were measured using an integrating sphere. [d]$k_r = \Phi/\tau$. [e]$k_{nr} = (1 - \Phi)/\tau$.

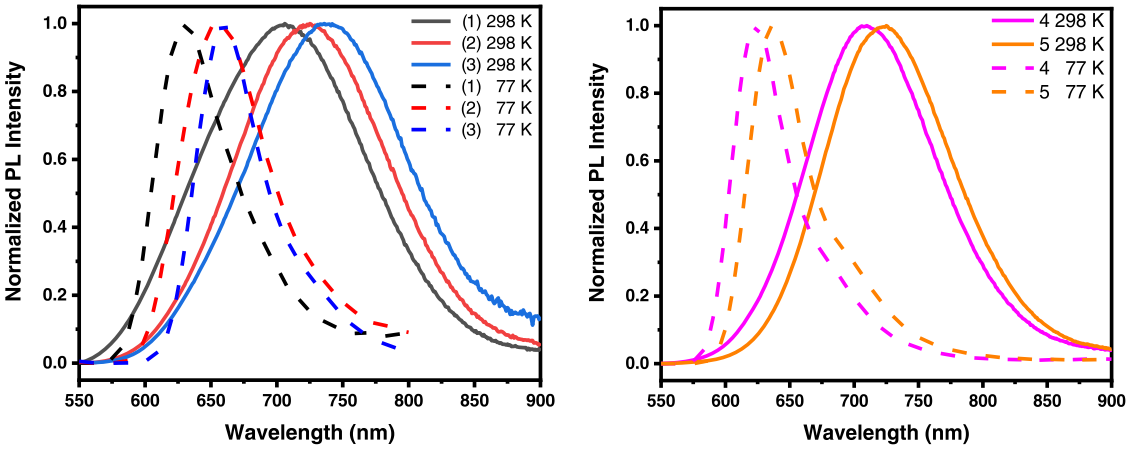

Figure 5. Left: PL spectra of the pyridine series at RT (solid line) and 77 K (dashed line) of **1** (black), **2** (red), and **3** (blue) (λ_{ex} = 500 nm). Right: PL spectra of the quinoline series at RT (solid line) and 77 K (dashed line) of **4** (magenta) and **5** (orange) (λ_{ex} = 500 nm). All spectra were recorded in toluene.

distances for these molecules to compare to our electronic structure calculations.[54,78]

Photoluminescence (PL) Spectroscopy. Consistent with the UV−vis spectra, the PL maxima red-shift in structures with greater d_{z^2} orbital overlap and easier to reduce cyclometalating ligands. The PL maxima of the thiolpyridine series measured in toluene at room temperature are 706 nm (**1**), 725 nm (**2**), and 736 nm (**3**), Figure 5 left. The only structural difference between **1** and **2** is the cyclometalating ligand, which alters the energy of the LUMO. The observed red-shift is attributed to decreasing LUMO energy when going from ppy to bzq, instead of increasing HOMO energy that is characteristically observed when the Pt−Pt distance is decreased. The only structural difference between **2** and **3** is the 6-methyl substituent on the bridging ligand. This increase of steric bulk near the coordination site has previously been used to decrease the observed Pt−Pt distance, therefore, raising the HOMO energy, culminating in a bathochromic of the PL spectrum. The PL maxima of the quinoline series echo that of their absorption spectra, with maxima at 710 nm (**4**) and 725 nm (**5**) in toluene, Figure 5 right. The decrease in PL energy between **4** and **5** can be attributed to the replacement of the cyclometalating ligand from ppy to bzq, which is consistent with the thiolpyridine series. The combined data suggest that the PL maxima of the dinuclear Pt(II) complex can be modulated by either using the coalescence of the two platinum centers induced by bridging ligand effects or using cyclometalating ligands with distinct reduction potentials. These

https://doi.org/10.1021/acs.inorgchem.1c02469
Inorg. Chem. XXXX, XXX, XXX−XXX

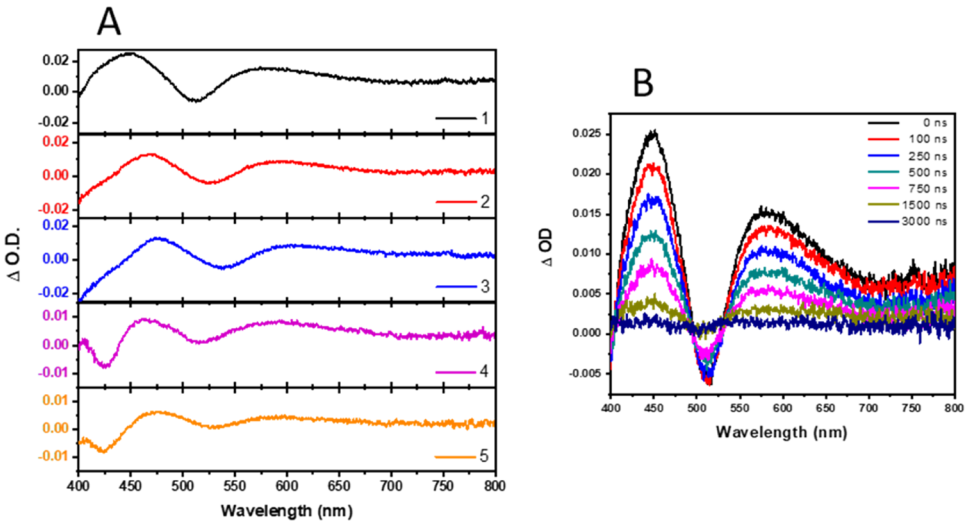

Figure 6. (A) Excited-state difference spectra of **1** (black), **2** (red), **3** (blue), **4** (magenta), and **5** (orange) in toluene measured promptly following 500 nm pulsed excitation (2 mJ/pulse, 7 ns full-width at half-maximum (FWHM)). The samples were deaerated using the freeze−pump−thaw technique. Each difference spectrum was measured promptly with a 10 ns gate width. (B) Excited-state absorption difference spectra measured for **1** as a function of delay time.

observations are again in line with the MMLCT charge-transfer character displayed in **1**−**5**.

When cooling the RT solution to 77 K in toluene, a rigidochromic blue-shift was measured in both series of dimers, Figure 5. The ordering of the excited-state energies remained consistent with those measured at RT. The magnitude of the thermally induced Stokes shift was larger in the quinoline series: 1915 cm^{-1} (**4**) and 1930 cm^{-1} (**5**) with respect to the pyridine series: 1665 cm^{-1} (**1**), 1475 cm^{-1} (**2**), and 1565 cm^{-1} (**3**). The magnitudes of the values for these measured thermally induced Stokes shifts align with the assignment of MMLCT excited states in these molecules.[79−81]

Single-exponential PL intensity decays were exhibited by the five molecules investigated, in deaerated toluene measured subsequent to 500 nm laser pulses (Figures S8, S9, and S38−S40); the corresponding photophysical parameters are presented in Table 2. The PL lifetimes of **1**−**5** are consistent with the MMLCT character, as observed previously for similar compounds.[54] The thiolpyridine series exhibits a decrease of the excited-state lifetime across the series from 1100 ns (**1**), 630 ns (**2**), and 510 ns (**3**) resulting from steady increases in the nonradiative decay rate constant (k_{nr}), consistent with the energy gap law. The thiolquinoline series has the opposite trend as the excited-state lifetimes increase from 100 ns (**4**) to 720 ns (**5**), resulting from a marked decrease in k_{nr} in going from **4** to **5** (Table 2).

Transient Absorption Spectroscopy. Nanosecond TA experiments were performed to explore the excited-state properties of these compounds and their prompt difference spectra are given in Figure 6. The difference spectrum of **1** exhibits absorption transients centered at 450 and 575 nm, having a minor ground-state bleach near 510 nm, consistent with the analogous 2-hydroxypyridyl bridged dimers.[54] The decay kinetics measured at different wavelengths were all self-consistent and quantitatively agreed with the corresponding PL decay kinetics (Table 2 and Figures S38−S40). The excited-state difference spectra of **2** and **3** feature absorption bands at 470 and 575 nm, a bleaching signal below 400 nm, concomitant with lower-energy bleaching signals centered at 525 nm (**2**) and 540 nm (**3**). Since the MMLCT transition is directed toward the cyclometalating ligands, the transient absorption features appear consistent for compounds having the same cyclometalating ligand as in molecules **2** and **3**. The excited-state difference spectra of **4** and **5** are blue-shifted in comparison to the thiolpyridine series. There are two absorption transients located at 460 and 600 nm and a bleaching signal at 425 nm. Molecules **1**−**5** generate transient features that are universally consistent with the generation of the radical anion of the cyclometalating moiety consistent with previously published molecules possessing MMLCT character.[54]

CONCLUSIONS

In summary, five Pt(II) dimers featuring ppy or bzq as cyclometalating ligands paired with either 2-thiolpyridine, 6-methyl-2-thiolpyridine, or 2-thiolquinoline were prepared and photophysically characterized. Unlike the corresponding pyrazole-bridged dimers containing identical C^N ligands, all of the thiolpyridine- and thiolquinoline-bridged dimers reported here were isolated exclusively as their anti-isomers and also exhibited low-energy absorption bands above 500 nm with MMLCT-based PL above 700 nm. The absolute PL quantum yields obtained for the molecules in this investigation ranged from 1 to 16%, which are notably larger than those based on the hydroxypyridine platform, whose PL quantum yields ranged from 0.33 to 3.97%.[54] Similarly, the thiolpyridine- and thiolquinoline-bridged dimers exhibit significantly longer excited-state lifetimes compared to the hydroxypyridine-bridged dimers, whose lifetimes are limited to hundreds of nanoseconds at RT. The combined data illustrate that pyridyl- and quinoline-thiolates in conjunction with ppy and bzq cyclometalates form classes of MMLCT chromophores with photophysical properties suitable for sensitizing bimolecular excited-state photochemical reactions. These molecules also enable systematic investigations of transient metal−metal interactions responsible for coherence phenomena in MMLCT chromophores.

https://doi.org/10.1021/acs.inorgchem.1c02469
Inorg. Chem. XXXX, XXX, XXX−XXX

■ ASSOCIATED CONTENT

Supporting Information

The Supporting Information is available free of charge at https://pubs.acs.org/doi/10.1021/acs.inorgchem.1c02469.

Experimental methods, structural characterization data, additional static and time-resolved spectra, additional electronic structure calculation details, and the 3D structures (*XYZ*) of **1**−**5** (PDF)

■ AUTHOR INFORMATION

Corresponding Author

Felix N. Castellano − *Department of Chemistry, North Carolina State University, Raleigh, North Carolina 27695-8204, United States;* orcid.org/0000-0001-7546-8618; Phone: (919) 515-3021; Email: fncastel@ncsu.edu

Authors

Subhangi Roy − *Department of Chemistry, North Carolina State University, Raleigh, North Carolina 27695-8204, United States*

Antonio A. Lopez − *Department of Chemistry, North Carolina State University, Raleigh, North Carolina 27695-8204, United States*

James E. Yarnell − *Department of Chemistry, North Carolina State University, Raleigh, North Carolina 27695-8204, United States;* orcid.org/0000-0003-0049-9887

Complete contact information is available at: https://pubs.acs.org/10.1021/acs.inorgchem.1c02469

Author Contributions

‡S.R. and A.A.L. contributed equally. The manuscript was written through contributions of all authors. All authors have given approval to the final version of the manuscript.

Notes

The authors declare no competing financial interest.

■ ACKNOWLEDGMENTS

This work was supported by the National Science Foundation (CHE-1955795). J.E.Y. was supported by the Air Force Institute of Technology (AFIT).

■ REFERENCES

(1) Connick, W. B.; Gray, H. B. Photooxidation of Platinum(II) Diimine Dithiolates. *J. Am. Chem. Soc.* **1997**, *119*, 11620−11627.

(2) Espinet, P.; Esteruelas, M. A.; Oro, L. A.; Serrano, J. L.; Sola, E. Transition metal liquid crystals: advanced materials within the reach of the coordination chemist. *Coord. Chem. Rev.* **1992**, *117*, 215−274.

(3) Evans, R. C.; Douglas, P.; Winscom, C. J. Coordination complexes exhibiting room-temperature phosphorescence: Evaluation of their suitability as triplet emitters in organic light emitting diodes. *Coord. Chem. Rev.* **2006**, *250*, 2093−2126.

(4) Ghedini, M.; Pucci, D.; Crispini, A.; Barberio, G. Oxidative Addition to Cyclometalated Azobenzene Platinum(II) Complexes: A Route to Octahedral Liquid Crystalline Materials. *Organometallics* **1999**, *18*, 2116−2124.

(5) Hissler, M.; McGarrah, J. E.; Connick, W. B.; Geiger, D. K.; Cummings, S. D.; Eisenberg, R. Platinum diimine complexes: towards a molecular photochemical device. *Coord. Chem. Rev.* **2000**, *208*, 115−137.

(6) Koo, C.-K.; Ho, Y.-M.; Chow, C.-F.; Lam, M. H.-W.; Lau, T.-C.; Wong, W.-Y. Synthesis and Spectroscopic Studies of Cyclometalated Pt(II) Complexes Containing a Functionalized Cyclometalating Ligand, 2-Phenyl-6-(1H-pyrazol-3-yl)-pyridine. *Inorg. Chem.* **2007**, *46*, 3603−3612.

(7) Lanoë, P.-H.; Fillaut, J.-L.; Toupet, L.; Williams, J. A. G.; Bozec, H. L.; Guerchais, V. Cyclometallated platinum(ii) complexes incorporating ethynyl−flavone ligands: switching between triplet and singlet emission induced by selective binding of Pb2+ ions. *Chem. Commun.* **2008**, 4333.

(8) Lu, W.; Mi, B.-X.; Chan, M. C. W.; Hui, Z.; Che, C.-M.; Zhu, N.; Lee, S.-T. Light-Emitting Tridentate Cyclometalated Platinum(II) Complexes Containing σ-Alkynyl Auxiliaries: Tuning of Photo- and Electrophosphorescence. *J. Am. Chem. Soc.* **2004**, *126*, 4958−4971.

(9) Ma, B.; Djurovich, P. I.; Yousufuddin, M.; Bau, R.; Thompson, M. E. Phosphorescent Platinum Dyads with Cyclometalated Ligands: Synthesis, Characterization, and Photophysical Studies. *J. Phys. Chem. C* **2008**, *112*, 8022−8031.

(10) McGarrah, J. E.; Kim, Y.-J.; Hissler, M.; Eisenberg, R. Toward a Molecular Photochemical Device: A Triad for Photoinduced Charge Separation Based on a Platinum Diimine Bis(acetylide) Chromophore. *Inorg. Chem.* **2001**, *40*, 4510−4511.

(11) Peyratout, C. S.; Aldridge, T. K.; Crites, D. K.; McMillin, D. R. DNA-Binding Studies of a Bifunctional Platinum Complex That Is a Luminescent Intercalator. *Inorg. Chem.* **1995**, *34*, 4484−4489.

(12) Siu, P. K. M.; Siu-Wai, L.; Lu, W.; Zhu, N.; Che, C.-M. A Diiminoplatinum(II) Complex of 4-Ethynylbenzo-15-crown-5 as a Luminescent Sensor for Divalent Metal Ions. *Eur. J. Inorg. Chem.* **2003**, *2003*, 2749−2752.

(13) Thomas, S. W.; Venkatesan, K.; Müller, P.; Swager, T. M. Dark-Field Oxidative Addition-Based Chemosensing: New Bis-cyclometalated Pt(II) Complexes and Phosphorescent Detection of Cyanogen Halides. *J. Am. Chem. Soc.* **2006**, *128*, 16641−16648.

(14) Wai-Yin Sun, R.; Ma, D.-L.; Wong, E. L.-M.; Che, C.-M. Some uses of transition metal complexes as anti-cancer and anti-HIV agents. *Dalton Trans.* **2007**, 4884.

(15) Wang, A. H. J.; Nathans, J.; Van Der Marel, G.; Van Boom, J. H.; Rich, A. Molecular structure of a double helical DNA fragment intercalator complex between deoxy CpG and a terpyridine platinum compound. *Nature* **1978**, *276*, 471−474.

(16) Wang, X.; Goeb, S. B.; Ji, Z.; Pogulaichenko, N. A.; Castellano, F. N. Homogeneous Photocatalytic Hydrogen Production Using π-Conjugated Platinum(II) Arylacetylide Sensitizers. *Inorg. Chem.* **2011**, *50*, 705−707.

(17) Wong, K. H.; Chan, M. C. W.; Che, C.-M. Modular Cyclometalated Platinum(II) Complexes as Luminescent Molecular Sensors for pH and Hydrophobic Binding Regions. *Chem.—Eur. J.* **1999**, *5*, 2845−2849.

(18) Wong, W.-Y.; He, Z.; So, S.-K.; Tong, K.-L.; Lin, Z. A Multifunctional Platinum-Based Triplet Emitter for OLED Applications#. *Organometallics* **2005**, *24*, 4079−4082.

(19) Zhang, D.; Wu, L.-Z.; Zhou, L.; Han, X.; Yang, Q.-Z.; Zhang, L.-P.; Tung, C.-H. Photocatalytic Hydrogen Production from Hantzsch 1,4-Dihydropyridines by Platinum(II) Terpyridyl Complexes in Homogeneous Solution. *J. Am. Chem. Soc.* **2004**, *126*, 3440−3441.

(20) Vezzu, D. A. K.; Deaton, J. C.; Jones, J. S.; Bartolotti, L.; Harris, C. F.; Marchetti, A. P.; Kondakova, M.; Pike, R. D.; Huo, S. Highly Luminescent Tetradentate Bis-Cyclometalated Platinum Complexes: Design, Synthesis, Structure, Photophysics, and Electroluminescence Application. *Inorg. Chem.* **2010**, *49*, 5107−5119.

(21) Chassot, L.; Mueller, E.; Von Zelewsky, A. cis-Bis(2-phenylpyridine)platinum(II) (CBPPP): a simple molecular platinum compound. *Inorg. Chem.* **1984**, *23*, 4249−4253.

(22) Constable, E. C.; Henney, R. P. G.; Leese, T. A.; Tocher, D. A. Cyclopalladated and cycloplatinated complexes of 6-phenyl-2,2′-bipyridine: platinum-platinum interactions in the solid state. *J. Chem. Soc., Chem. Commun.* **1990**, 513−515.

(23) Che, C.-M.; Fu, W.-F.; Lai, S.-W.; Hou, Y.-J.; Liu, Y.-L. Solvatochromic response imposed by environmental changes in matrix/chromophore entities: luminescent cyclometalated platinum-

(ii) complex in Nafion and silica materials. *Chem. Commun.* **2003**, 118−119.
(24) Lu, W.; Chan, M. C. W.; Cheung, K.-K.; Che, C.-M. $\pi-\pi$ Interactions in Organometallic Systems. Crystal Structures and Spectroscopic Properties of Luminescent Mono-, Bi-, and Trinuclear Trans-cyclometalated Platinum(II) Complexes Derived from 2,6-Diphenylpyridine. *Organometallics* **2001**, *20*, 2477−2486.
(25) Cárdenas, D. J.; Echavarren, A. M.; Ramírez De Arellano, M. C. Divergent Behavior of Palladium(II) and Platinum(II) in the Metalation of 1,3-Di(2-pyridyl)benzene. *Organometallics* **1999**, *18*, 3337−3341.
(26) Jude, H.; Krause Bauer, J. A.; Connick, W. B. Tuning the Electronic Structures of Platinum(II) Complexes with a Cyclometalating Aryldiamine Ligand. *Inorg. Chem.* **2004**, *43*, 725−733.
(27) Rausch, A. F.; Thompson, M. E.; Yersin, H. Triplet state relaxation processes of the OLED emitter Pt(4,6-dFppy)(acac). *Chem. Phys. Lett.* **2009**, *468*, 46−51.
(28) Ma, B.; Djurovich, P. I.; Thompson, M. E. Excimer and electron transfer quenching studies of a cyclometalated platinum complex. *Coord. Chem. Rev.* **2005**, *249*, 1501−1510.
(29) Brooks, J.; Babayan, Y.; Lamansky, S.; Djurovich, P. I.; Tsyba, I.; Bau, R.; Thompson, M. E. Synthesis and Characterization of Phosphorescent Cyclometalated Platinum Complexes. *Inorg. Chem.* **2002**, *41*, 3055−3066.
(30) Miller, J. S.; Epstein, A. J. One-Dimensional Inorganic Complexes. In *Progress in Inorganic Chemistry*; Lippard, S. J., Ed.; John Wiley & Sons, Inc., 1976; pp 1−151.
(31) Novoa, J. J.; Aullon, G.; Alemany, P.; Alvarez, S. On the Bonding Nature of the M.cntdot..cntdot..cntdot.M Interactions in Dimers of Square-Planar Pt(II) and Rh(I) Complexes. *J. Am. Chem. Soc.* **1995**, *117*, 7169−7171.
(32) Schindler, J. W.; Fukuda, R. C.; Adamson, A. W. Photophysics of aqueous tetracyanoplatinate(2-). *J. Am. Chem. Soc.* **1982**, *104*, 3596−3600.
(33) Saito, D.; Ogawa, T.; Yoshida, M.; Takayama, J.; Hiura, S.; Murayama, A.; Kobayashi, A.; Kato, M. Intense Red-Blue Luminescence Based on Superfine Control of Metal-Metal Interactions for Self-Assembled Platinum(II) Complexes. *Angew. Chem., Int. Ed.* **2020**, *59*, 18723−18730.
(34) Law, A. S. Y.; Lee, L. C. C.; Yeung, M. C. L.; Lo, K. K. W.; Yam, V. W. W. Amyloid Protein-Induced Supramolecular Self-Assembly of Water-Soluble Platinum(II) Complexes: A Luminescence Assay for Amyloid Fibrillation Detection and Inhibitor Screening. *J. Am. Chem. Soc.* **2019**, *141*, 18570.
(35) Chaaban, M.; Zhou, C.; Lin, H.; Chyi, B.; Ma, B. Platinum(II) binuclear complexes: molecular structures, photophysical properties, and applications. *J. Mater. Chem. C* **2019**, *7*, 5910−5924.
(36) Saito, K.; Nakao, Y.; Sakaki, S. Theoretical Study of Pyrazolate-Bridged Dinuclear Platinum(II) Complexes: Interesting Potential Energy Curve of the Lowest Energy Triplet Excited State and Phosphorescence Spectra. *Inorg. Chem.* **2008**, *47*, 4329.
(37) Koshiyama, T.; Omura, A.; Kato, M. Redox-controlled Luminescence of a Cyclometalated Dinuclear Platinum Complex Bridged with Pyridine-2-thiolate Ions. *Chem. Lett.* **2004**, *33*, 1386−1387.
(38) Aoki, R.; Kobayashi, A.; Chang, H.-C.; Kato, M. Structures and Luminescence Properties of Cyclometalated Dinuclear Platinum(II) Complexes Bridged by Pyridinethiolate Ions. *Bull. Chem. Soc. Jpn.* **2011**, *84*, 218−225.
(39) Ma, B.; Li, J.; Djurovich, P. I.; Yousufuddin, M.; Bau, R.; Thompson, M. E. Synthetic Control of Pt···Pt Separation and Photophysics of Binuclear Platinum Complexes. *J. Am. Chem. Soc.* **2005**, *127*, 28−29.
(40) Chakraborty, A.; Deaton, J. C.; Haefele, A.; Castellano, F. N. Charge-transfer and ligand-localized photophysics in luminescent cyclometalated pyrazolate-bridged dinuclear platinum(II) complexes. *Organometallics* **2013**, *32*, 3819−3829.
(41) Rachford, A. A.; Castellano, F. N. Thermochromic Absorption and Photoluminescence in [{Pt(ppy)(μ-Ph2pz)}2]. *Inorg. Chem.* **2009**, *48*, 10865.
(42) Lockard, J. V.; Rachford, A. A.; Smolentsev, G.; Stickrath, A. B.; Wang, X.; Zhang, X.; Atenkoffer, K.; Jennings, G.; Soldatov, A.; Rheingold, A. L.; Castellano, F. N.; Chen, L. X. Triplet Excited State Distortions in a Pyrazolate Bridged Platinum Dimer Measured by X-ray Transient Absorption Spectroscopy. *J. Phys. Chem. A* **2010**, *114*, 12780−12787.
(43) McCusker, C. E.; Chakraborty, A.; Castellano, F. N. Excited State Equilibrium Induced Lifetime Extension in a Dinuclear Platinum(II) Complex. *J. Phys. Chem. A* **2014**, *118*, 10391−10399.
(44) Han, M.; Tian, Y.; Yuan, Z.; Zhu, L.; Ma, B. A Phosphorescent Molecular "Butterfly" that undergoes a Photoinduced Structural Change allowing Temperature Sensing and White Emission. *Angew. Chem., Int. Ed.* **2014**, *53*, 10908−10912.
(45) Zhou, C.; Yuan, L.; Yuan, Z.; Doyle, N. K.; Dilbeck, T.; Bahadur, D.; Ramakrishnan, S.; Dearden, A.; Huang, C.; Ma, B. Phosphorescent Molecular Butterflies with Controlled Potential-Energy Surfaces and Their Application as Luminescent Viscosity Sensor. *Inorg. Chem.* **2016**, *55*, 8564−8569.
(46) Zhou, C.; Tian, Y.; Yuan, Z.; Han, M.; Wang, J.; Zhu, L.; Tameh, M. S.; Huang, C.; Ma, B. Precise Design of Phosphorescent Molecular Butterflies with Tunable Photoinduced Structural Change and Dual Emission. *Angew. Chem., Int. Ed.* **2015**, *54*, 9591−9595.
(47) Chaaban, M.; Chi, Y.-C.; Worku, M.; Zhou, C.; Lin, H.; Lee, S.; Ben-Akacha, A.; Lin, X.; Huang, C.; Ma, B. Thiazol-2-thiolate-Bridged Binuclear Platinum(II) Complexes with High Photoluminescence Quantum Efficiencies of up to Near Unity. *Inorg. Chem.* **2020**, *59*, 13109−13116.
(48) Sicilia, V.; Borja, P.; Martín, A. Half-Lantern Pt(II) and Pt(III) Complexes. New Cyclometalated Platinum Derivatives. *Inorganics* **2014**, *2*, 508.
(49) Arnal, L.; Fuertes, S.; Martin, A.; Baya, M.; Sicilia, V. A Cyclometalated N-Heterocyclic Carbene: The Wings of the First Pt2(II, II) Butterfly Oxidized by CHI3. *Chem.—Eur. J.* **2018**, *24*, 18743.
(50) Fuertes, S.; Chueca, A. J.; Martin, A.; Sicilia, V. New NHC Cycloplatinated Compounds. Significance of the Cyclometalated Group on the Electronic and Emitting Properties of Biscyanide Compounds. *J. Organomet. Chem.* **2019**, *889*, 53.
(51) Arnal, L.; Fuertes, S.; Martin, A.; Sicilia, V. The Use of Cyclometalated NHCs and Pyrazoles for the Development of Fully Efficient Blue PtII Emitters and Pt/Ag Clusters. *Chem.—Eur. J.* **2018**, *24*, 9377.
(52) Sicilia, V.; Arnal, L.; Fuertes, S.; Martin, A.; Baya, M. Metal-Metal Cooperation in the Oxidation of a Flapping Platinum Butterfly by Haloforms: Experimental and Theoretical Evidence. *Inorg. Chem.* **2020**, *59*, 12586−12594.
(53) Sicilia, V.; Arnal, L.; Escudero, D.; Fuertes, S.; Martin, A. Chameleonic Photo- and Mechanoluminescence in Pyrazolate-Bridged NHC Cyclometalated Platinum Complexes. *Inorg. Chem.* **2021**, *60*, 12274−12284.
(54) Chakraborty, A.; Yarnell, J. E.; Sommer, R. D.; Roy, S.; Castellano, F. N. Excited-State Processes of Cyclometalated Platinum-(II) Charge-Transfer Dimers Bridged by Hydroxypyridines. *Inorg. Chem.* **2018**, *57*, 1298−1310.
(55) Saito, K.; Hamada, Y.; Takahashi, H.; Koshiyama, T.; Kato, M. Organic Light-Emitting Diodes Based on a Binuclear Platinum(II) Complex. *Jpn. J. Appl. Phys.* **2005**, *44*, L500−L501.
(56) Saito, K.; Nakao, Y.; Umakoshi, K.; Sakaki, S. Theoretical Study of Excited States of Pyrazolate- and Pyridinethiolate-Bridged Dinuclear Platinum(II) Complexes: Relationship between Geometries of Excited States and Phosphorescence Spectra. *Inorg. Chem.* **2010**, *49*, 8977−8985.
(57) Shahsavari, H. R.; Lalinde, E.; Moreno, M. T.; Niazi, M.; Kazemi, S. H.; Abedanzadeh, S.; Barazandeh, M.; Halvagar, M. R. Half-lantern cyclometalated Pt(ii) and Pt(iii) complexes with bridging heterocyclic thiolate ligands: synthesis, structural characterization, and

https://doi.org/10.1021/acs.inorgchem.1c02469
Inorg. Chem. XXXX, XXX, XXX−XXX

electrochemical and photophysical properties. *New J. Chem.* **2019**, *43*, 7716−7724.
(58) Zhu, Y.; Luo, K.; Zhao, L.; Ni, H.; Li, Q. Binuclear platinum(II) complexes based on 2-mercaptobenzothiazole 2-mercaptobenzimidazole and 2-hydroxpyridine as brigding ligands: Red and near-infrared luminescence originated from MMLCT transition. *Dyes Pigm.* **2017**, *145*, 144−151.
(59) Kim, P.; Kelley, M. S.; Chakraborty, A.; Wong, N. L.; Van Duyne, R. P.; Schatz, G. C.; Castellano, F. N.; Chen, L. X. Coherent Vibrational Wavepacket Dynamics in Platinum(II) Dimers and Their Implications. *J. Phys. Chem. C* **2018**, *122*, 14195−14204.
(60) Ishikawa, T.; Hayes, S. A.; Keskin, S.; Corthey, G.; Hada, M.; Pichugin, K.; Marx, A.; Hirscht, J.; Shionuma, K.; Onda, K.; Okimoto, Y.; Koshihara, S.-y.; Yamamoto, T.; Cui, H.; Nomura, M.; Oshima, Y.; Abdel-Jawad, M.; Kato, R.; Miller, R. J. D. Direct observation of collective modes coupled to molecular orbital−driven charge transfer. *Science* **2015**, *350*, 1501.
(61) Craig, C. A.; Garces, F. O.; Watts, R. J.; Palmans, R.; Frank, A. J. Luminescence properties of two new Pt(II)-2-phenylpyridine complexes; the influence of metal-carbon bonds. *Coord. Chem. Rev.* **1990**, *97*, 193−208.
(62) Mdleleni, M. M.; Bridgewater, J. S.; Watts, R. J.; Ford, P. C. Synthesis, Structure, and Spectroscopic Properties of Ortho-Metalated Platinum(II) Complexes. *Inorg. Chem.* **1995**, *34*, 2334−2342.
(63) Lai, S.-W.; Chan, M. C. W.; Cheung, K.-K.; Peng, S.-M.; Che, C.-M. Synthesis of Organoplatinum Oligomers by Employing N-Donor Bridges with Predesigned Geometry: Structural and Photophysical Properties of Luminescent Cyclometalated Platinum(II) Macrocycles. *Organometallics* **1999**, *18*, 3991−3997.
(64) Barboy, N.; Feitelson, J. Deoxygenation of solutions for transient studies. *Anal. Biochem.* **1989**, *180*, 384−386.
(65) Pavlishchuk, V. V.; Addison, A. W. Conversion constants for redox potentials measured versus different reference electrodes in acetonitrile solutions at 25 °C. *Inorg. Chim. Acta* **2000**, *298*, 97−102.
(66) Frisch, M. J.; Trucks, G. W.; Schlegel, H. B.; Scuseria, G. E.; Robb, M. A.; Cheeseman, J. R.; Scalmani, G.; Barone, V.; Petersson, G. A.; Nakatsuji, H.; Li, X.; Caricato, M.; Marenich, A.; Bloino, J.; Janesko, B. G. *Gaussian 09*, revision D.01; Gaussian, Inc.: Wallingford, CT, 2009.
(67) Becke, A. D. A new mixing of Hartree−Fock and local density-functional theories. *J. Chem. Phys.* **1993**, *98*, 1372−1377.
(68) Becke, A. D. Density-functional thermochemistry. III. The role of exact exchange. *J. Chem. Phys.* **1993**, *98*, 5648−5652.
(69) Zhao, Y.; Truhlar, D. G. The M06 suite of density functionals for main group thermochemistry, thermochemical kinetics, noncovalent interactions, excited states, and transition elements: two new functionals and systematic testing of four M06-class functionals and 12 other function. *Theor. Chem. Acc.* **2008**, *120*, 215−241.
(70) Adamo, C.; Barone, V. Toward reliable density functional methods without adjustable parameters: The PBE0 model. *J. Chem. Phys.* **1999**, *110*, 6158−6170.
(71) Weigend, F.; Ahlrichs, R. Balanced basis sets of split valence, triple zeta valence and quadruple zeta valence quality for H to Rn: Design and assessment of accuracy. *Phys. Chem. Chem. Phys.* **2005**, *7*, 3297.
(72) Andrae, D.; Häußermann, U.; Dolg, M.; Stoll, H.; Preuß, H. Energy-adjusted ab initio pseudopotentials for the second and third row transition elements. *Theor. Chim. Acta* **1990**, *77*, 123−141.
(73) Cossi, M.; Scalmani, G.; Rega, N.; Barone, V. New developments in the polarizable continuum model for quantum mechanical and classical calculations on molecules in solution. *J. Chem. Phys.* **2002**, *117*, 43−54.
(74) Grimme, S.; Antony, J.; Ehrlich, S.; Krieg, H. A consistent and accurate ab initio parametrization of density functional dispersion correction (DFT-D) for the 94 elements H-Pu. *J. Chem. Phys.* **2010**, *132*, No. 154104.
(75) Haldrup, K.; Dohn, A. O.; Shelby, M. L.; Mara, M. W.; Stickrath, A. B.; Harpham, M. R.; Huang, J.; Zhang, X.; Møller, K. B.; Chakraborty, A.; Castellano, F. N.; Tiede, D. M.; Chen, L. X. Butterfly Deformation Modes in a Photoexcited Pyrazolate-Bridged Pt Complex Measured by Time-Resolved X-Ray Scattering in Solution. *J. Phys. Chem. A* **2016**, *120*, 7475−7483.
(76) Kulikova, M. V.; Balashev, K. P.; Kvam, P. I.; Songstad, J. Effects of the Nature of the Ligand Environment and Metal Center on the Optical and Electrochemical Properties of Platinum(II) and Palladium- (II) Ethylenediamine Complexes with Heterocyclic Cyclometalated Ligands. *Russ. J. Gen. Chem.* **2000**, *70*, 163−170.
(77) Ma, B.; Djurovich, P. I.; Garon, S.; Alleyne, B.; Thompson, M. E. Platinum Binuclear Complexes as Phosphorescent Dopants for Monochromatic and White Organic Light-Emitting Diodes. *Adv. Funct. Mater.* **2006**, *16*, 2438−2446.
(78) Brown-Xu, S. E.; Kelley, M. S. J.; Fransted, K. A.; Chakraborty, A.; Schatz, G. C.; Castellano, F. N.; Chen, L. X. Tunable Excited-State Properties and Dynamics as a Function of Pt−Pt Distance in Pyrazolate-Bridged Pt(II) Dimers. *J. Phys. Chem. A* **2016**, *120*, 543−550.
(79) Pomestchenko, I. E.; Castellano, F. N. Solvent Switching between Charge Transfer and Intraligand Excited States in a Multichromophoric Platinum(II) Complex. *J. Phys. Chem. A* **2004**, *108*, 3485−3492.
(80) Pomestchenko, I. E.; Luman, C. R.; Hissler, M.; Ziessel, R.; Castellano, F. N. Room Temperature Phosphorescence from a Platinum(II) Diimine Bis(pyrenylacetylide) Complex. *Inorg. Chem.* **2003**, *42*, 1394−1396.
(81) Whittle, C. E.; Weinstein, J. A.; George, M. W.; Schanze, K. S. Photophysics of Diimine Platinum(II) Bis-Acetylide Complexes. *Inorg. Chem.* **2001**, *40*, 4053−4062.

https://doi.org/10.1021/acs.inorgchem.1c02469
Inorg. Chem. XXXX, XXX, XXX−XXX